BIOCHEMISTRY
including biophysical chemistry & molecular biology

ARTICLE

pubs.acs.org/biochemistry

Light-Induced Conformational Changes in Photosynthetic Reaction Centers: Redox-Regulated Proton Pathway near the Dimer

Sasmit S. Deshmukh,[†] JoAnn C. Williams,[‡] James P. Allen,[‡] and László Kálmán*[,†]

[†]Department of Physics, Concordia University, Montreal, Quebec H4B 1R6, Canada

[‡]Department of Chemistry and Biochemistry, Arizona State University, Tempe, Arizona 85287-1604, United States

Supporting Information

ABSTRACT: The influence of the hydrogen bonds on the light-induced structural changes were studied in the wild type and 11 mutants with different hydrogen bonding patterns of the primary electron donor of reaction centers from *Rhodobacter sphaeroides*. Previously, using the same set of mutants at pH 8, a marked light-induced change of the local dielectric constant in the vicinity of the dimer was reported in wild type and in mutants retaining Leu L131 that correlated with the recovery kinetics of the charge-separated state [Deshmukh et al. et al. (2011) Biochemistry, 50, 340−348]. In this work after prolonged illumination the recovery of the oxidized dimer was found to be multiphasic in all mutants. The fraction of the slowest phase, assigned to a recovery from a conformationally altered state, was strongly pH dependent and found to be extremely long at room temperature, at pH 6, with rate constants of $\sim 10^{-3}$ s^{-1}. In wild type and in mutants with Leu at L131 the very long recovery kinetics was coupled to a large proton release at pH 6 and a decrease of up to 79 mV of the oxidation potential of the dimer. In contrast, in the mutants carrying the Leu to His mutation at the L131 position, only a negligible fraction of the dimer exhibited lowered potential, the large proton release was not observed, the oxidized dimer recovered 1 or 2 orders of magnitude faster depending on the pH, and the very long-lived state was not or barely detectable. These results are modeled as arising from the loss of a proton pathway from the bacteriochlorophyll dimer to the solvent when His is present at the L131 position.

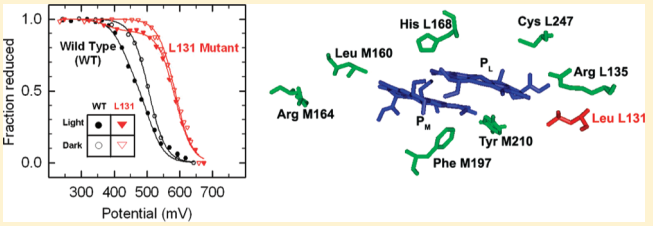

The reaction center (RC) of photosynthetic purple bacteria provides a scaffold to bind redox carriers that perform electron transfer reactions, resulting in a light-induced transmembrane charge separation.[1] A key element of efficient biological electron transfer is the fine-tuning of the redox potentials of donor−acceptor pairs that set the driving force for each electron transfer step.[2] In proteins or *in vitro*, the redox potential of similar or even the same cofactors can be very different. For example, the *in situ* redox potentials of the primary electron donors of photosystem II and the bacterial RC differ by 0.6−0.9 V[3−5] despite a difference of the redox potentials of only 0.1 V in organic solvents.[6] Also, the potential difference of two identical ubiquinone-50 molecules (Q_A and Q_B) that serve as the terminal electron acceptors within the same protein in the bacterial RC is ∼60 mV, pointing out the importance of the differences in the dielectric properties of the local protein environment.[1] The bacterial RC is a pigment−protein complex that noncovalently binds the pigment cofactors in the two subunits termed L and M.[7] The primary electron donor (P) in *Rhodobacter (Rba.) sphaeroides* is a dimer of two bacteriochlorophyll *a* molecules (labeled as P_L and P_M) that are about 3.5 Å apart. Overwhelming structural and spectroscopic evidence demonstrates that in the wild type (WT) and in the carotenoidless R-26 mutant only the 2-acetyl group of P_L is engaged in a hydrogen-bond (H-bond) with the surrounding protein.[8−12] The 9-keto groups of ring E could serve as proton acceptors for H-bonds, but in the WT RC the adjacent Leu residues at the L131 and M160 positions are not capable of donating protons. These positions were targeted to construct a series of mutants where new H-bonds were formed between the 9-keto groups of P_L and P_M by replacing the Leu residues with His at the L131 and M160 positions, respectively. Similarly, the replacement of the Phe with a His at the M197 position resulted in a new H-bond with the 2-acetyl group of P_M. The H-bond that exists in the WT between the L168 His and the 2-acetyl group of P_L has been removed by the replacement of this His with a Phe residue. The combination of these mutations at these four sites resulted in more than a dozen mutants that span an unprecedented 350 mV range for the potential of the dimer.[5] The influence of the H-bonds on the electron transfer was extensively studied in the past.[10−13]

This study of the slow conformational rearrangements upon illumination was inspired by the pioneering work of Kleinfeld and colleagues.[14] Many groups have followed their path in the past quarter of a century and provided new insights to the details of these changes.[15−21] Despite these extensive efforts, the exact molecular mechanisms of such conformational changes are still

Received: February 2, 2011
Revised: March 15, 2011
Published: March 16, 2011

not clear. The spectral features are consistent with structural rearrangements involving amino acid residues and bound water molecules near P, with L131 playing a critical role.[21] Most groups have targeted the acceptor side of the RC primarily because structural changes were present upon illumination near Q_B and the H-subunit.[22,23] These crystallographic studies, however, used very short (<1 s) illuminations to generate the light-adapted structures in crystals and may not be fully relevant to studies using minute scale illuminations and structural changes taking place in the minute time scale.

Very recently, we reported light-induced electrochromic absorption changes that were attributed to a marked increase of the local dielectric constant near P.[21] The extent of the change of the dielectric constant was found to be strongly dependent on the identity of the residue occupying the L131 position. In this study, experiments are performed to understand the characteristics of the light-induced long-lived charge separated and conformational states and the nature of the involvement of L131. The combination of light-induced optical spectroscopy, electrochemical redox, and protonational measurements are used here to identify the characteristics of the conformational states, in particular the energetics and protonational states.[21] These features are discussed in terms of the involvement of a slow proton pathway from the primary donor.

EXPERIMENTAL PROCEDURES

Mutagenesis, Bacterial Growth, and RC Isolation. The construction of the mutant strains of *Rba. sphaeroides* by oligonucleotide-directed mutagenesis has been described earlier.[24−26] The strains were grown under nonphotosynthetic conditions, and the RCs were isolated using procedures according to Williams and coworkers.[25] The RCs were kept in 15 mM MES, Hepes, Tris-HCl, bis-tris-propane, or MOPS depending on the pH. The RCs were dispersed in 0.1% lauryldimethylamine oxide (LDAO) and 1 mM EDTA, except the samples for electrochemical redox titration and proton uptake/release measurements (see below). The purity of the RCs, defined as the ratio of the absorbance at 280 to 802 nm, was between 1.2 and 1.5 for all preparations used in this study. Using LDAO as a detergent to study RCs under continuous illumination was chosen based upon extensive studies that used this combination successfully.[10,12,14,15,17,18,20,21]

Optical Spectroscopy. Near-infrared (700−1000 nm) optical spectra and the kinetics of the absorbance changes on the minute time scale were measured using a Cary 5000 spectrophotometer from Varian (Mulgrave, Victoria, Australia). The formation of light-induced states was achieved by external, continuous wave excitation using a 250 W tungsten lamp (Oriel 6129). The exciting light was delivered from the lamp to the samples using a high throughput fiber optics (Newport Corp., Irvine, CA). An interference filter with maximum transmittance at 850 ± 20 or 870 ± 20 nm was mounted on the fiber optics. The light intensity was set to ~30% of the saturating value for wild type at a 2 μM RC concentration. Terbutryne was used at a concentration of 100 μM to eliminate secondary quinone activity. Laser flash induced absorption changes were recorded with a miniaturized laser flash photolysis (LFP-112) system equipped with a near-infrared sensitive photomultiplier (Luzchem Research Inc., Ottawa, Canada). The kinetics were analyzed by decomposition of the recorded traces into exponentials using Marquardt nonlinear least-squares method. All measurements were performed at room temperature.

Spectroelectrochemical Redox Titrations. The oxidation−reduction midpoint potential of the P/P^+ couple was determined by spectroelectrochemical oxidation−reduction titration both in the dark and under a weak continuous, external illumination. For these measurements the ionic detergent, LDAO, was replaced with a nonionic detergent, Triton X-100 (TX-100), and the EDTA was removed by ion exchange chromatography and a 24 h dialysis, respectively.[5] The intensity of the illumination was selected to achieve the bleaching of 3−7% of the dimer only depending on the mutants. This very weak illumination prevented the samples from suffering photo damage during the long experiments and also ensured that the vast majority of the dimer is in its reduced state at any given time without an applied potential. The angle of the illumination was ~45° with respect to the propagation of the monitoring beam to avoid stray light entering the detector chamber. The degree of the electrochemical oxidation of P was determined by monitoring the absorption at the maximum of the Q_y band centered at 865 nm in WT from the near-infrared (700−1000 nm) spectra recorded at different ambient redox potentials with a Cary 5000 spectrophotometer as described earlier.[3,5] The ambient redox potential was adjusted with a CV-27 potentiostat from Bioanalytical Systems (West Lafayette, IN), and the RCs were placed into a thin-layer spectroelectrochemical cell of local design containing a 333 lines/in. gold mesh (Precision Eforming, Cortland, NY), similar to a system described earlier.[3] A miniature calomel electrode (Cole Palmer, Vernon Hills, IL) was used as the reference electrode. The calibration of the calomel electrode potential was done according to O'Reilly.[27] Potassium hexacyanoferrate-(II) and potassium tetracyanomono(1,10-phenanthroline)ferrate-(II) were added in 300 μM concentration as redox mediators. The data were fitted with a one-electron Nernst equation as described earlier.[5] During the measurements conducted under and within a certain time interval after weak illumination two populations of P had been observed with two different midpoint potentials and two components were used instead of one. The RCs for the electrochemical titrations were concentrated to ~300 μM and were kept in 0.05% TX-100, 1 mM EDTA, 15 mM MES, Tris-HCl, or MOPS depending on the pH. All measurements were performed at room temperature.

Proton Uptake/Release Measurements. For these measurements the ionic detergent LDAO was replaced by 0.05% TX-100 by using ion-exchange column chromatography to eliminate the buffering capacity caused by the protonatable groups of LDAO. Then the buffer (15 mM Tris-HCl) and the EDTA were removed by a long (24−48 h) dialysis, with frequent changing of the dialysing medium (0.05% TX-100, 100 mM NaCl, pH 8.0). The ionic strength of the assay solution was kept constant by 100 mM NaCl to ensure a stable reading. Light-induced pH changes were measured by an Orion Ross semimicro combination pH electrode connected to an Orion 920A precision pH meter (Thermo Scientific). The net proton uptake or release was the difference of the electrode responses between the unbuffered (~1 μM) and buffered (15 mM) samples. To determine the buffering capacity of the entire system, a known amount of strong acid (HCl) was added during extensive stirring of the sample solution. All measurements were performed at room temperature.

RESULTS

Kinetics of Formation and Recovery of Light-Induced States at Different pH Values. The kinetics of the absorption changes caused by 1 min illumination with subsaturating light

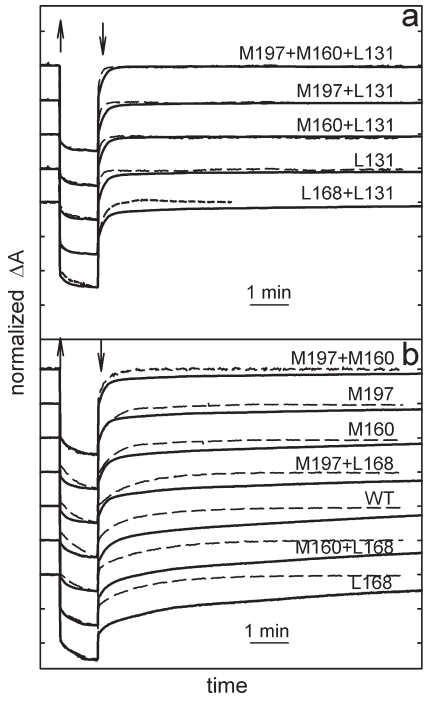

Figure 1. Formation and disappearance of the light-induced redox states in the wild type and 11 hydrogen bonding mutants measured at the position of the dimer band at pH 6 (continuous lines) and at pH 8 (dashed lines) using 1 min illumination. Panel a: mutants containing the Leu to His substitution at L131. Panel b: all other mutants and WT. The traces were normalized and vertically shifted for better comparison. The vertical up and down arrows indicate when the illumination was turned on and off, respectively.

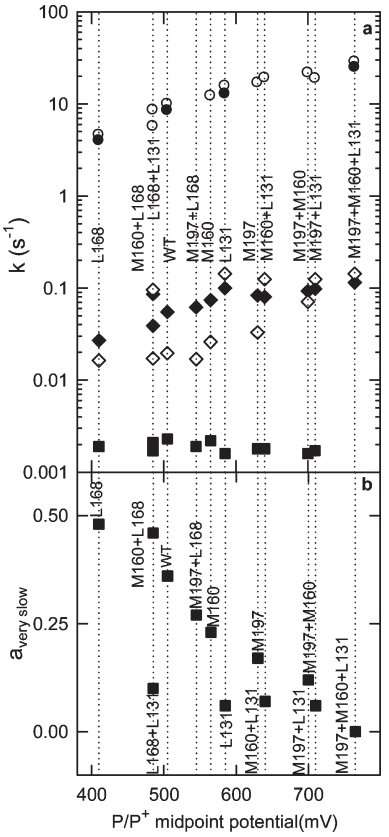

Figure 2. Dependence of the kinetic parameters obtained from the recovery kinetics of the oxidized dimer on the P/P^+ potential. Panel a: rate constants of the flash induced charge recombination (circles) and the slow (diamonds) and very slow (squares) components in the 1 min illumination induced recovery kinetics. Open and closed symbols refer to the data obtained from the exponential fitting of the kinetic traces recorded at pH 8 and 6, respectively. Panel b: amplitude of the very slow component at pH 6.

intensity was measured at the center of the Q_y band of P in each mutant and the WT at pH 6 and 8 (Figure 1). Under the applied conditions, in the presence of terbutryne, the $P^+Q_A^-$ state was formed immediately. In addition to the unresolved, rapid absorption change, a further slower increase of the signal was also observed in all RCs at both pH values. The slow increase of the signal was interpreted to be arising from altered populations of the RCs generated by the continuous illumination. After the illumination was turned off complex recoveries were detected with two or three components that had much different lifetimes than those observed after single flash excitation. The number of components, their relative amplitudes, and their lifetimes were strongly dependent on the pH at the given illumination time. As the illumination was turned off in a fraction of the RCs a rapid, unresolved recovery was observed. This fast recovery was attributed to the $P^+Q_A^- \rightarrow PQ_A$ charge recombination from the dark-adapted conformation. The additional slower components were assigned to the recoveries from different light-induced conformations. As seen in Figure 1, the overall recovery kinetics were much longer at pH 6 than at pH 8 in WT and one set of the mutants, whereas in another set of mutants, all of which contain the Leu to His substitution at the L131 position, the kinetics appeared only slightly longer than at pH 8. All RCs exhibited reversible signals with the applied 1 min illumination. Longer illumination times (>3 min) resulted in a slight degree of photodamage at pH 6 in the mutants with a highly oxidizing P such as the M197 + M160 + L131 and the M197 + L131 mutants. The recovery kinetics with the applied illumination conditions at pH 8 were predominately biphasic, while at pH 6 in all mutants except in the M197 + M160 + L131 mutant a third, very slow component was also detected. The rate constants of the slow and very slow components for pH 6 and 8 are plotted in Figure 2a as a function of the midpoint potential of the P/P^+ couple that has been determined earlier for dark-adapted samples.[5] From laser flash photolysis the rate constants of the flash-induced charge recombination are also plotted for reference for all mutants at pH 8 and for a few representatives for pH 6. The values measured at pH 8 are in agreement with those reported earlier.[5] The rate constants of the flash-induced charge recombination from Q_A^- to P^+ were found to be very weakly dependent on pH in the mutants. This agrees with the conclusions of former studies conducted in WT and R-26.[28] The rate constants of the slow component at pH 8 both in the mutants with H-bonds at the L131 position and in those that lack the H-bond at the L168 position were found to be independent of the P/P^+ midpoint potential.[21] The values of the rate constants for these two families of mutants, however, were about 7−8 times larger in the L131 family than in the L168 family with the most extreme values of 1.4×10^{-1} and 1.6×10^{-2} s^{-1}, respectively. At pH 6 the rate constants for the slow component were found to be faster than at pH 8 in the mutants that lack the H-bond at L131. For example in

the WT this increase is almost 3-fold from 2.0×10^{-2} s^{-1} at pH 8 to 5.5×10^{-2} s^{-1} at pH 6. The rate constants of the very slow component at pH 6, which was not detectable at pH 8, after 1 min illumination, was found also to be independent of the P/P^+ potential in all mutants with a small variation between 1.6×10^{-3} and 2.3×10^{-3} s^{-1} in the 11 studied RCs. This component was not populated to detectable level in the M197 + M160 + L131 triple mutant. These observations suggest that most likely the conformational state represented by the very slow component is formed in a consecutive reaction from the state characterized with the slow component. In general, the total amplitudes of the slower phases were larger at pH 6 than at pH 8, especially in the family of mutants that lack the L131 His substitution. The relative amplitude of the very slow component, however, is only 6−7% in most of the mutants in the L131 family and only 10% in the L168 + L131 mutant that, although having the H-bond at the L131 position, lacks the one at the L168 position (Figure 2b). Contrarily, in the mutants that lack the H-bond at the L131 position the relative amplitude of this very slow component varied from as high as 48% in the L168 mutant that lacks any H-bond to 12% in the M197 + M160 mutant with three H-bonds.

Potential of the P/P^+ Couple in the Light-Induced States. The results of the spectroelectrochemical redox titrations at pH 8 for the WT and for the L168 and L131 mutants in the dark and in the presence of a weak external illumination are presented in Figure 3. Without any external illumination the data could be fitted well with a single Nernst equation assuming only one population of P with midpoint potentials of 505, 415, and 585 mV for the WT and for the L168 and the L131 mutants, respectively. The error was estimated as ±7 mV based on the results obtained from different titrations in the dark. These values determined here are in a good agreement with those reported earlier for the P/P^+ potentials in WT and in these mutant RCs.[5]

Normally, the P/P^+ midpoint potential is determined under dark conditions using dark-adapted samples as described above, with the potential being adjusted either chemically or electrochemically while optically monitoring the amount of P and P^+ present at each potential. Each measurement intrinsically takes few minutes in order for the protein to equilibrate with the applied potential, usually with the inclusion of mediators. The kinetics of this equilibration both in the dark and in the presence of a weak illumination is shown in Figure S1 of the Supporting Information as the bleaching of the P-band at 865 nm in response to the onset and offset of +600 mV applied potential. Since the mediators are applied at nearly equimolar concentrations with the RCs, they are not expected to serve as electron donors/acceptors in a second-order process to P^+ or P, but their absence results in much longer equilibration times in both directions (data not shown). The same kinetics for the equilibration in the presence and in the absence of the weak illumination verifies that neither the RCs nor the mediators respond differently to the potential change and that the response does not depend on the conformational state of the protein. The titrations in the dark reveal the midpoint potential of the P^+ state relative to the ground state exclusively in the dark-adapted conformation of the RC. When the experiments were performed in the presence of weak illumination, it resulted in only a few percent of the RCs being present in the charge-separated state, but the RCs in the ground state were preferentially enriched in the light-adapted conformation rather than being only in the dark-adapted conformation. Thus, the measurements shown in Figure 3 resulted in two apparent

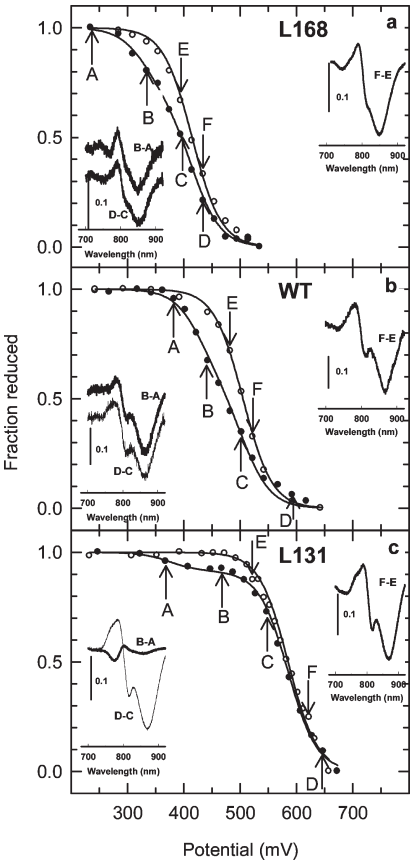

Figure 3. Spectroelectrochemical oxidation−reduction titrations of RCs from WT, the L168, and the L131 mutant at pH 8. Open symbols represent the data obtained in dark-adapted samples, and the closed symbols represent the data determined in the presence of weak illumination. The continuous lines are the best fits to the Nernst equation with one (open symbols) or two (closed symbols) components with different potentials. The insets show difference spectra between two absolute spectra recorded at two different applied potential values indicated by the arrows and letters from A to F. Conditions, errors, and the results of the fit are described in the text and in Figure 4.

midpoint potentials, corresponding to the two populations of P in RCs with two different conformations.

While in the larger fraction of the RCs the midpoint potential of the P/P^+ couple did not change in the presence of the weak illumination, in the smaller fraction significantly lower values were determined in all RCs. In the WT upon illumination the potential of the dimer was shifted to 430 mV in 42% of the RCs representing a 75 mV drop in the potential (Figure 3b). Similarly, a 79 mV difference was obtained in the L168 mutant for the P/P^+ potentials with values of 415 and 336 mV for the dark-adapted and light-adapted populations, respectively (Figure 3a). The fraction of the component with lower dimer potential slightly varied 27−31% and 41−45% in different measurements for the L168 mutant and WT, respectively, most probably due to the different positioning of the samples within the spectroelectrochemical cell resulting in slightly altered illumination conditions for the individual measurements. Contrarily, in the L131 mutant only 8% of P exhibited altered potentials with a value of 375 mV in the presence of the illumination. We would like to stress that even though it is obvious from Figure 3c that a two-component Nernst fit is required to describe the measured data well even in

the L131 mutant due to the very small amplitude for this component the error of the potential is ±32 mV as opposed to the error of ±7 mV for the WT and the L168 mutant at pH 8. Applying a single-component Nernst fit for the L131 mutant yielded a value of 577 mV for the P/P^+ potential (data not shown). The insets in Figure 3 show the P^+/P difference spectra determined as the differences of the absolute spectra recorded at two specific applied potentials (labeled as A−F) situated at different regimes of the Nernst curves. It is clearly visible from these insets that in the WT and in the L168 mutant the difference spectra in the dark (F−E) are very similar to those fractions of the samples that had the same potential in the light (D−C). The difference spectra that represent the population of P with lower potential values (B−A) show smaller electrochromic absorption changes around 800 nm. This observation is in line with the conclusions of our recently published work,[21] where during the illumination similar decreases of the electrochromic absorption changes of the bacteriochlorophyll monomer (B) bands were observed in RCs that exhibited longer recovery kinetics after illumination. The decrease of the electrochromic absorption changes were attributed to light-induced structural changes, which increase the local dielectric constant and are responsible for the altered P/P^+ potential. In Figure 3c, the insets for the L131 mutant show the similarities of the spectra obtained in the dark (F−E) and the major component determined during the weak illumination (D−C), but for the 8% component the difference spectrum is quite dissimilar. It exhibits the electrochromic red shift in the range of the B bands but has very little contribution from P^+. Overall, this difference spectrum in the L131 mutant resembles the double difference spectrum obtained as the difference between two light-minus-dark difference spectra recorded after different illumination times.[21] As the electrochemical titrations cannot probe the photoinduced P^+, only those that were generated by the electrical potential, these measurements suggest that even after the charges recovered heterogeneity exists in the RCs. Figure S2 of the Supporting Information shows the near-infrared optical difference spectra recorded at various times up to 7 h after the weak illumination was turned off. The reference spectrum for these measurements was the one that was recorded in the dark prior to the illumination. Even though the spectral signatures of both P^+ and Q_A^- disappeared in WT within an hour after a prolonged illumination the electrochromic absorption changes around 800 nm, which were indicative of the altered local dielectric constant,[21] remained until 5 h after the light was turned off. Similar, long-lasting spectral features were reported earlier for RCs dispersed in LDAO[17,18] and in *n*-dodecyl-*β*-D-maltoside,[19] indicating that the detergents have no influence on these electrochromic absorption changes. The spectroelectrochemical titrations were also performed in this 7 h dark relaxation in two different time intervals. The titration that was conducted between 1 and 3.5 h after the light was turned off still showed the presence of two different populations of P in accordance with the presence of the electrochromic changes. The fraction of the P with altered potential, however, decreased from 42% to 26% in WT compared to the value determined during the illumination (Figure S3, Table S1). When the redox titration was conducted between approximately 6.5 and 8.0 h after the illumination was turned off, where the electrochromic changes were not present in the spectra anymore, the data could be described with a single-component Nernst fit with 501 mV midpoint potential for P, as was found before the illumination (Figure S3, Table S1). Comparison of Figures S2 and S3 shows

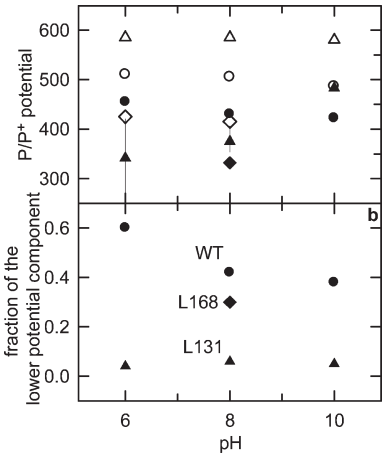

Figure 4. Panel a: pH dependence of the P/P^+ potential for WT (circles), the L168 mutant (diamonds), and the L131 mutant (triangles). The potential values determined in the dark and in the presence of weak external illumination are shown with open and filled symbols, respectively. Experimental errors are within the sizes of the symbols unless indicated by vertical lines. Panel b: pH dependence of the amplitude of the component with lowered P/P^+ potential determined from the titrations performed under weak illumination. Conditions: ∼300 *μ*M RCs, 70 mM KCl, 300 *μ*M mediators in 0.05% TX-100.

that the fraction of the RCs with an altered redox potential for P disappeared with the same kinetics as the electrochromic absorption changes involving the monomers, indicating that the source for the altered potential of P is the light-induced change of the dielectric constant.

The P/P^+ midpoint potentials were also determined at pH 6 and 10 and were plotted in Figure 4a. In the dark the P/P^+ potentials followed very weak pH dependences corresponding to ∼−6 mV/pH and ∼−1 mV/pH slopes as the pH is raised from pH 6 to 10 in the WT and in the L131 mutant, respectively. In the L168 mutant a trend very similar to WT was observed between pH 6 and 8 as the P/P^+ potential is increased from 415 to 425 mV while the pH was lowered from 8 to 6. In the presence of a weak illumination the decrease of the P/P^+ potential was comparable with the ones measured at pH 8 with values of 55 and 64 mV at pH 6 and 10, respectively. The amplitude of the fraction that exhibited lowered potential in WT, however, increased to 60% at pH 6 and was found to be 38% at pH 10 compared to the 42% at pH 8 (Figure 4b). Contrarily, in the L131 mutant this fraction did not change at pH 10 and decreased at pH 6 to the detection limit of 4% from the value of 8% found at pH 8, making the error of determining the P/P^+ potential for this small component as large as ±80 mV at pH 6.

Proton Release. Proton uptake/release measurements were performed in RCs from WT and the L131 mutant at pH 6 using prolonged, 5 min illumination (Figure 5a). This longer illumination was necessary to reach the saturation values of the proton signals in the set up used for this measurement. After a 5 min illumination, in the WT a large proton release, with ∼6.5 H^+/RC was observed. This value is in very good agreement with the proton release reported earlier for the R-26 strain at pH 6.[16] In the L131 mutant, only a small release of ∼0.3 H^+/RC was detected that may correspond to a ∼5% fraction of the RCs trapped in the longest-lived light-induced conformation. For both samples, the recovery of the proton release followed the recovery kinetics of the optical signals corresponding to the

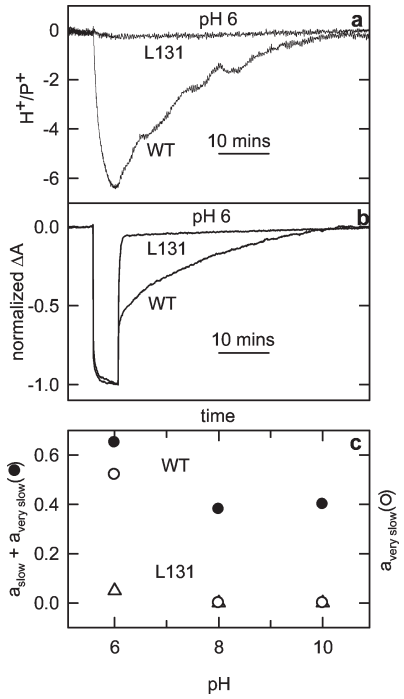

Figure 5. Kinetics of the light-induced proton release (a) and absorption changes (b) in WT and in the L131 mutant at pH 6. The traces for panel a are the differences between the unbuffered and the strongly buffered measurements. Conditions for panel a: 2 μM RCs in 0.05% TX-100, 100 mM NaCl, 100 μM terbutryne; for the buffered signal +15 mM MES. Conditions for panel b: same as for panel a except 0.1% LDAO instead of TX-100. Illumination time: 5 min through 870 ± 15 nm interference filter using water bath as a heat filter. Panel c: pH dependence of the amplitude of the trapped states in the recovery kinetics of the absorption changes.

longest-lived states measured under the same 5 min illumination (Figure 5b). For better comparison, the light-induced kinetic traces were also recorded using a 5 min illumination. In the recovery kinetics after the light was turned off the amplitude of the slowest component increased from 35% to 60% in WT at pH 6 as the illumination time increased from 1 to 5 min (see Figure 1 for comparison). The rate constant of the longest-lived component on the other hand dropped only from 2.3×10^{-3} to 1×10^{-3} s^{-1} as the illumination time was increased by 5-fold. The observed kinetics in WT for prolonged illumination recorded here in LDAO is very similar to those found in the carotenoid-less mutant strain R-26 measured in TX-100.[16] The matching kinetics of the proton release measured in TX-100 (Figure 5a) and the optical signals recorded in LDAO (Figure 5b) for WT and in TX-100 for R-26 indicate that these two detergents do not alter the proposed structural changes or the redox states of the RCs. The kinetics of the L131 mutant at pH 6 remained almost the same as was seen at 1 min illumination. The vast majority of the RCs (95%) recovered immediately, and only the remaining 5% featured the long recovery. At pH 8 even the longer, 5 min illumination could not generate the component with the rate constant of $\sim 10^{-3}$ s^{-1} either in the WT or in the L131 mutant. Consequently, only a $\sim$0.4 H^+/RC proton release was observed in WT at pH 8 with the 5 min illumination (data not shown). The pH dependence of the relative extent of the slow and very slow components in WT and in the L131 mutant is displayed in Figure 5c and shows

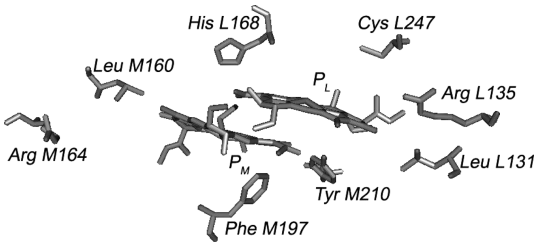

Figure 6. Structure of the bacteriochlorophyll dimer P and nearby amino acid residues Leu L131, Leu M160, His L168, and Phe M197. Alteration of each of these residues results in different patterns of hydrogen bonding to P. The residues with protonatable side chains, Arg L135, Cys L247, Arg M164, and Tyr M210 are also shown. Coordinates were taken from PDB entry code 4RCR.[7]

remarkable similarities to those that have been obtained from the spectroelectrochemical redox titrations for the fraction with lowered potential P (Figure 4b).

DISCUSSION

Light-induced changes that take place on relatively long time scales were studied in RCs from WT and a series of mutants. The work presented here is the direct continuation of our recent study conducted using the same set of mutants and the WT.[21] In the mutants P has various different H-bonding patterns with the surrounding protein environment that has been established by histidine substitutions near the 2-acetyl and the 9-keto groups of the two halves of P (Figure 6). In this work we have detected a $\sim$75 mV drop of the midpoint potential of P upon illumination in one family of mutants that lacks the H-bond between the L131 His and the 9-keto group of P_L. In these mutants and WT the decrease of the potential was accompanied by long lifetimes of the charge-separated state at any pH and a release of $\sim$6 H^+ at pH 6. Neither of these features was detectable after flash excitation. The relationship between the recovery kinetics of the $P^+Q_A^-$ charge pair, the light-induced protonational changes, and the redox midpoint potential of the P/P^+ couple after prolonged continuous illumination is discussed.

Origins of the Light-Induced Decrease of the Dimer Potential. Earlier studies indicated that the introduction of the H-bonds with His residues as proton donors at the M160, M197, and L131 positions increased the redox midpoint potential of the P/P^+ couple between 65 and 125 mV at pH 8 depending on the position.[5] Similarly, the removal of the H-bond found in the WT by substituting the L168 His with a Phe residue caused a 95 mV drop of the potential in the L168 mutant. Multiple substitutions have an additive effect on the potential, resulting in a 350 mV range for the potential of P between the lowest and the highest potential mutant. The redox midpoint potential of the P/P^+ couple determined in the presence of a weak illumination showed that in the absence of the His residue at the L131 position the illumination caused the potential of the dimer to decrease by 75−79 mV in a large fraction of WT and the L168 mutant at pH 8 (Figures 3 and 4). In contrast, in the presence of the His at the L131 position only a marginal fraction of the RCs exhibited a decreased dimer potential.

Such a large change in the potential of P should originate from either within the bacteriochlorophyll molecules or from their immediate vicinity. In a very recently published work, where we studied the same set of mutants and the WT, we reported that the

light-induced structural changes noticeably altered the local dielectric constant near P in WT and in mutants that show long recovery kinetics after continuous illumination but not in the mutants that contained the Leu to His replacement at the L131 position.[21] The change of the redox potential upon the alteration of the dielectric constant is expected. For example, the difference in the *in situ* redox midpoint potentials of the same ubiquinone-10 molecule in RCs occupying the hydrophobic, buried Q_A and the water accessible, polar, Q_B binding sites is ~60 mV (reviewed in ref 1). The P/P^+ potential was shown to be regulated in mutants by the protonational state of introduced Asp and Glu residues to the M199 and L170 and L168 positions, situated within 6 Å from P.[29] A potential drop of ~60 mV was observed when the pH was elevated from 6.0 to 9.5, corresponding to a loss of one positive charge through the deprotonation of these Asp and Glu side chains in those mutants. In the WT RC there are very few amino acids with protonational side chains in the immediate vicinity of P (Figure 6). Under normal circumstances the positively charged Arg residues at the L135 and M164 positions are expected to have high pK_a values that should be outside the investigated pH range. In the presence of the positive charge on P about 10 Å away, however, the pK_a values may be shifted downward to values that fall into the investigated range. If replaced by neutral residues the P/P^+ potentials were reported to drop by 12−24 mV in dark-adapted RCs for the L135 and M164 positions, respectively.[30] The pK_a of the L247 Cys in light-adapted samples was determined to be 8.7 in a tyrosine oxidizing mutant where this residue serves as a proton acceptor to the Tyr L167 residue.[31] Tyr M210 is considered to be one of the key residues in the initial electron transfer process in RC. Upon its replacement to Trp, Phe, or Leu the initial charge separation drastically slowed down, and the redox potential of the P/P^+ couple in the dark was elevated by up to 50 mV.[32,33] Indirect evidence indicates that if the Trp residue is substituted at the M210 position in mutants with very high P/P^+ potentials that were designed to utilize Tyr residues at various positions as electron donors to P^+, the P/P^+ potential did not drop during continuous illumination.[34,35] The assumption of a deprotonation-mediated stabilization of P^+ requires the P/P^+ potential to be strongly dependent on pH for the light-adapted conformations provided the protons are in equilibrium with the surrounding solution and the pK_a shifts are small.[29] If, however, the interaction energy between the oxidized P and the deprotonating residue is high, then the pK_a shift could be several pH units and the pH dependence should be moderate (ref 36, Figure 4). Tyr M210 is in van der Waals contact with P_M, and the effective local dielectric constant was reported to be only 1.5−4.7 times larger than vacuum.[37] These conditions are extremely favorable to a large pK_a shift upon the oxidation of P. For example, near Q_B in a medium with an effective dielectric constant of ~20, the pK_a of the Glu L212 was reported to be upshifted by ~4 pH units to 9.8 due to the negative charge on the Asp L213 residue ~5 Å away.[38] The light-induced change in the local dielectric constant not only should alter the P/P^+ potential but also the pK_a values of the nearby residues, since the interaction energies between the charges are inversely proportional to the dielectric constant. For example, the difference in the oxidation potentials of various quinones in organic solvents and *in situ* at the Q_A binding site showed a several hundred millivolts difference, demonstrating the strong dependence of the potential values on the dielectric properties of the environment.[39] The observed 75 mV drop in the potential of the P/P^+ couple and its moderate pH dependence in WT upon prolonged illumination is consistent with the deprotonation of one very close residue plus one or more that have weaker interaction with the dimer. The most likely candidate for the strongly interacting residue is Tyr M210. Whether or not the deprotonation can take place and the released protons can reach the solvent or they are only delivered away from P is dependent upon the existence of a proton conducting pathway that extends from P to the surface. The proton transfer has very slow kinetics of proton release and the accompanying optical changes. This inefficiency is consistent with the proton pathway in WT being not efficient, presumably because it is not physiologically relevant due to the normally fast reduction of P^+ by cytochrome in the cell. A large number of buried protonatable side chains have been reported to equilibrate with the solvent in the minute time scale.[40] Several slow proton conducting pathways were characterized in mutants that were designed to oxidize nearby Tyr residues by P^+ at positions L135, M164, and L167.[31,34,41,42] The delivery or the trapping of the released phenolic protons were sensitive to the identity of the introduced proton acceptors and the pH. When a His is introduced at L131, the data are consistent with the loss of this proton pathway between Tyr M210 and the surrounding and ultimately the solvent. The loss of the pathway has several consequences for the properties of P^+. The slow kinetics seen in the optical and proton release measurements of WT are now eliminated as the protons can no longer be transferred away from P^+, resulting in only the rapid optical changes being evident. In WT, the long-lived state has a lower P/P^+ midpoint potential due to the redistribution of charges near P, with a loss of positive charge, but for L131 mutants the protons can no longer carried away and there is no redistribution or redox change. The light-induced change of the local dielectric constant upon continuous illumination was reported to be much smaller in these mutants than those found in WT.[21] The proton pathway presumably involves water molecules rather than just amino acid side chains. The potential role of the structural water molecules near P in facilitating the structural changes was discussed in detail recently.[21] Two of these five structural water molecules (W736, W237) are very close to P, and one (W723) is very close to Leu L131, while all are within 7 Å distance from P. The introduction of His at the L131 does not allow the decrease of the P/P^+ potential that leads to rapid recovery kinetics. A complementary explanation for the observed light-induced decrease of the P/P^+ potential also assumes the involvement of Tyr M210 and can address why the continuous illumination is unable to drive the entire population of the RC to the long-lived state. Even though the heterogeneous population of the RC after continuous illumination was observed in all previous studies, this problem was not scrutinized. Situating within H-bond distance from the 2-acetyl group of P_M Tyr M210 initially was modeled to be engaged in a H-bond, but later this assumption was dismissed.[33,43] The 2-acetyl group of P_M was also modeled to be a potential ligand to the central Mg^{2+} of P_L both in *Rba. sphaeroides* and earlier in *Blastochloris viridis*.[44,45] These reports suggest the possibility of an axial ligand switch between the L173 His and the 2-acetyl group of P_M to maintain the pentacoordination of the Mg^{2+}, which is reported to be favored in proteins.[46] A ligation of the 2-acetyl group of P_M with the central Mg^{2+} of P_L or an H-bond with Tyr M210 with comparable probabilities could explain why the continuous illumination generated two major populations of the RCs and was unable to drive the entire RC population to the long-lived state even after prolonged

illumination. Both the ligation to the Mg^{2+} of P_L and the H-bond to Tyr M210 would force the 2-acetyl group out of the molecular plane and thus would not result in the change of the spin density distribution and the position of the Q_y absorption band of P.[47] In the presence of the H-bond between the His at the L131 position and the 9-keto group of P this switch is disrupted, and a rapid recovery is observed without stabilization of P^+. Redox-induced conformational changes were reported in other proteins as well, for example in the sensor domain of Ec DOS protein and in receptor protein−tyrosine phosphatase.[48,49]

Recovery Rates. In the mutants the rate constants of the $P^+Q_A^- \rightarrow PQ_A$ charge recombination after flash excitation followed the dependence on the midpoint potential as expected from the Marcus theory.[2,5] The pH dependence of the P/P^+ potential was reported to be very weak with only about −5 mV/pH slope between pH 6 and 10.[50] Thus, the differences in the Marcus behavior should not be significant at different pH values (see Figure 1 for few representative mutants). In this work the use of prolonged continuous illumination, however, generated redox states in fractions of the RCs whose recovery kinetics no longer followed the classical Marcus dependence for the rate constants. In the two groups of mutants the rate constants for the slower phases were mostly independent of the midpoint potential of the dimer, indicating that the observed rate must be limited by another factor, e.g., the rate of protonation or a conformational change. Because some of these mutants have larger rate constants than other mutants with similar midpoint potentials, the presence of the Leu to His mutation at L131 is consistent with an increase in the electron transfer rate, so that the electron transfer rate is significantly faster than the observed rate. Several groups reported the multiphasic recovery kinetics associated with light-induced conformational changes in the minutes time scale, but very few of them studied their pH dependencies.[14−20] The observed rate constants for the slower components at pH 8 agree well with those reported in these earlier studies for similar illumination times. As the illumination time increases new, longer-lived states were identified in the kinetic traces, resulting in some changes in the rate constants of the recovery kinetics.[20] This indicates that some later conformational states are formed from the earlier ones as a result of consecutive reactions. For example, the observation of the very slow component with the rate constant of $\sim 10^{-3}$ s^{-1} at pH 6 also resulted in the nearly 3-fold increase of the rate constant of the slow component from 2.0×10^{-2} at pH 8 to 5.5×10^{-2} s^{-1} at pH 6. The stoichiometry of the light-induced proton release at pH 6 correlates with the amplitude of the very slow component that could not have been observed at pH 8 (Figure 5). The conformational state with a large proton release at pH 6 could only be built up significantly in the mutants that showed longer recovery kinetics, exhibited decreases in their P/P^+ potential, and showed decreased electrochromic absorption changes in the B bands.[21] The agreement between the kinetics of the recovery of proton release and the recovery of the charge separated state at pH 6 is even more pronounced if we compare these data with those reported earlier for R-26.[19]

Assigning the Kinetic Components to Conformational Changes. Most of the earlier conformational studies argued that the origin of the long-lived states upon continuous illumination must stem from conformational changes near the quinones.[15,17−20] This assumption was supported by structural studies where indeed electron density changes were observed upon illumination near Q_B and the H-subunit.[22,23] These X-ray crystallographic studies used, however, very short (<1 s) illuminations to generate the light-induced states as the crystals would not diffract if exposed to longer illuminations.[23,51] It is obvious from this work as well as earlier illumination time-dependent analyses that accumulation of the really long-lived states requires a much longer illumination time than 1 s.[16,20] We present a model (Scheme 1) that explains the results of this work and our recently published study[21] with a minimum of assumptions. In the scheme the horizontal displacements are redox reactions ($D \rightarrow L_0$) and deprotonational steps ($L_H \rightarrow L_0$), and the vertical displacements are structural changes between conformational levels (L1 → L2 → L3) from a dark-adapted conformation (L1), to an intermediate light-adapted conformation (L2), and to the final light-adapted conformation (L3). In dark-adapted samples (L1) the charge separation forms the $P^+Q_A^-$ state, and in the vast majority of the samples charge recombination takes place in the ∼30−100 ms time scale depending on the pH and the mutants (Figure 2). Because of the very low quantum yield of the conformational changes, multiple turnovers are needed to build up the different conformational levels indicated by L2 and L3. The multiple turnovers can be achieved either by continuous illumination or trains of flashes as suggested in earlier studies.[14−21] The populations of the different conformational levels are dependent upon the illumination time and the mutation. At very short illumination times (∼1 s) the component with a rate constant of $\sim 10^{-1}$ s^{-1} is the first to appear in the recovery kinetics among the slower components in the WT, and this component was predominantly observed even after longer illuminations in the mutants containing His at L131 (at level L2) besides the normal charge recombination. It can also be seen in virtually all mutants if another component with a similar rate constant does not mask it (Figure 2). When the reduced quinone was rapidly oxidized

Scheme 1. Minimal Model of the Light-Induced and Redox Reactions, Conformational, and Protonational Changes in RCs[a]

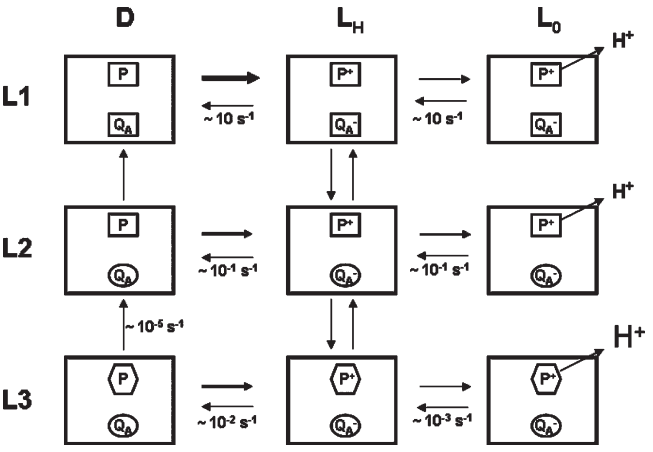

[a] The RCs are shown as large rectangles. The dark-adapted conformations for both P and Q_A are shown as small rectangles, and the different light-adapted conformations of the protein in the vicinity of P and Q_A are indicated with hexagons and ellipses, respectively. The horizontal changes indicate charge separation (→) and charge recombination (←) from the dark (D) to under light (L_H) and the protonational changes between the protonated (L_H) and the deprotonated (L_0) forms of the RCs are also shown with horizontal arrows. The approximate rate constants for the recovery processes are indicated near the corresponding arrows. A full description is found in the text.

by excess ferricyanide after a flash excitation, P^+ has been reported to scavenge an electron from the surroundings with a rate constant of $\sim 10^{-1}$ s^{-1} in R-26 and also in *Blastochoris viridis* RCs.[16,50,52] If an early light-induced conformational change around the quinones blocks the return of the electron to P^+, one can assume a similar situation. Thus, we propose that the component with a rate constant of $\sim 10^{-1}$ s^{-1} is most likely due to the recovery of P^+ caused by the light-induced conformational changes taking place in the vicinity of the quinones, at the cytoplasmic side of the RC. This assignment is in agreement with the X-ray crystallographic studies where after short illuminations (<1 s) structural changes were only reported near the quinones and in the H-subunit.[22,23] While the L2 level appears to be populated for WT and all mutants, significant population of L3 is observed only for WT and mutants with the native Leu at L131. The component with rate constants of $\sim 10^{-2}$ s^{-1} (at level L3) was only observed in the mutants that exhibited a large decrease of the P/P^+ potential (Figures 2 and 3) and was also accompanied by decreased electrochromic absorption changes of the bacteriochlorophyll monomer band upon illumination that was assigned to the increase of the local dielectric constant.[21] It should be noted that in the mutants with the M197 Phe to His substitution the recovery kinetics were the fastest in their group (Figure 1), but they were not as rapid as in the L131 family of mutants and exhibited some degree of dependence on the P/P^+ potential (ref 21, Figure 2). This is consistent with the models presented above since the M197 His is close to both the 2-acetyl group of P_M and Tyr M210 (Figure 6). We assigned the L3 level as the conformational state formed due to structural changes occurring at the periplasmic side, near P. As the amplitude of the very slow component with a rate constant of $\sim 10^{-3}$ s^{-1} at pH 6 was correlated with the extent of the proton release and was predominantly detected in the mutants that lack the L131 His, we conclude that this component should also arise from conformational changes at the periplasmic side but from a different protonational state. The matching kinetics of the recovery of the proton release (Figure 5a) and the recovery of the charge-separated state (Figure 5b) indicates that the reprotonation step is rate limiting at the L3 level. After flash excitation, at the L1 level, the kinetics of the reuptake of the substoichiometric proton release was also found to be the same as the charge recombination.[50] The unusual, large proton release that has also been reported earlier for R-26 was attributed to the different pK_as of several protonatable residues near the periplasmic surface in the light- and dark-adapted conformations of the RC.[16] Since the proton release is not coupled with additional decrease of neither the P/P^+ potential nor the electrochromic absorption changes of the monomer bands, most of the proton releasing residues must not be in the immediate vicinity of P or the B monomers. It has been discussed earlier that there are a total of 14 Glu, Asp, and His (not ligated) residues that are at least 10 Å away from P on the periplasmic side of the RC and may have their pK_a values in the acidic pH range and can account for the 6.5 H^+/RC proton release here in WT and for the 6.0 H^+/RC in R-26 reported earlier.[16] The increase of the local dielectric constant was shown to shift the pK_a values of the side chains of the acidic residues downward and those of the basic residues upward in globular proteins.[53] Because around pH 6 the Asp and Glu residues are more likely expected to undergo protonational changes than the basic ones, the observed proton release in WT and in R-26 is in agreement with the decrease of the pK_as of the 14 possible acidic residues. It was shown earlier that even after flash excitation proton release from near P^+ can only be observed at low pH values.[36,50] This indicates that the pK_a values of the residues near P should be below pH 8 and explains why in this work and after flash excitation proton release was only observed at low pH and not at pH 8. The $L_H \rightarrow L_0$ deprotonation step in Scheme 1 is therefore strongly pH dependent in all conformations. While the proton release in the dark-adapted conformation (at level L1) after a single flash excitation is also caused by the shift of the pK_as of the nearby residues, it can only be substoichiometric since it is due to the interaction of the single positive charge on P with the protonatable side chains.[36,50] This can only provide very moderate stabilization for P^+ due to proton release. At level L3, however, the increased value of the dielectric constant can shift the pK_as of many residues, significantly resulting in a large proton release and almost an order of magnitude longer lifetime of the charge-separated state.

According to the proposed Scheme 1, there are two different conformations of P: the dark-adapted conformation at levels L1 and L2 (indicated by squares) and the light-adapted conformation, at level L3 (shown as hexagons). The relaxation time from L3 to the L2 (or L1) conformational level in the ground state was found to be ~6 h (rate constant of $\sim 10^{-5}$ s^{-1}) after prolonged illumination (Figure S2) and about 1 h after 1 min illumination.[21] These conformational states are the sources for the two populations of P with different redox potentials in WT and in mutants with Leu at L131 (Figure 3 and Figure S3). As level L3 is not populated significantly in the mutants containing the His at L131, P predominantly exists only in the dark-adapted conformation (at levels L1 and L2) in these mutants (Figure 3 and Figure S3, Table S1).

In summary, we have shown that the rate of the recovery of the oxidized dimer in the $P^+Q_A^-$ state depends systematically on the protein environment of P^+. In particular, replacement of the Leu to His at the L131 position appears to prevent the light-induced conformational changes that result in a very slow recovery of the charge-separated state, the drop of the P/P^+ potential, and a large proton release at pH 6. These events correlate with the extent of the light-induced change in the local dielectric constant near P.[21] The long-lived P^+ cannot be generated by electrochemical oxidation alone even in the light-adapted conformation (Figure S1) as it requires the presence of the electric field between Q_A^- and P^+ established by the light-induced charge separation and the subsequent structural changes that have low quantum yields. We have also shown that the kinetics of the light-induced conformational changes and the proton release in WT are very similar to those reported earlier in the carotenoid-less R-26 mutant, and they are independent of the detergents used.[16] The extension of the lifetime of the charge-separated state by up to 4 orders of magnitude via light-induced structural and protonational changes provides new opportunities to utilize the RCs in energy storage as biocapacitors. The charges separated by a low dielectric medium can be prevented from recombination by systematic alteration of the environment of the charges, and the light can be used as a switch. Experiments to increase the lifetime of the $P^+Q_A^-$ state even further are underway.

■ ASSOCIATED CONTENT

Supporting Information. Kinetics of the spectroelectrochemical oxidation and reduction of the dimer in the presence and the absence of weak illumination monitored at 865 nm as the response to the onset and offset of +600 mV potential; difference spectra of the WT RC recorded at different times (up to 7 h) after the weak illumination is turned off (these spectra feature the

disappearance of the light-induced electrochromic absorption changes of the bacteriochlorophyll monomers in the dark); spectroelectrochemical redox titrations of P conducted during different time intervals before, during, and after the prolonged weak illumination; fitting parameters of the Nernst equation for the redox titrations of P. This material is available free of charge via the Internet at http://pubs.acs.org.

AUTHOR INFORMATION

Corresponding Author

*Phone: 514-848-2424 x5051. Fax: 514-848-2828. E-mail: laszlo.kalman@concordia.ca.

Funding Sources

This work was supported by grants from Natural Sciences and Engineering Research Council of Canada (to L.K.) and from National Science Foundation (MCB 0640002 to J.P.A.).

ABBREVIATIONS

RC, reaction center; P, bacteriochlorophyll dimer; Q_A, primary quinone; Q_B, secondary quinone; WT, wild type; H-bond, hydrogen bond; LDAO, lauryldimethylamine oxide; TX-100, Triton X-100; *Rba*, *Rhodobacter*.

REFERENCES

(1) Hunter, C. N., Daldal, F., Thurnauer, M. C., Beatty, J. T., Eds. (2008) *The Purple Phototropic Bacteria*, Springer-Verlag, Dordrecht, The Netherlands.

(2) Marcus, R. A., and Sutin, N. (1985) Electron transfers in chemistry and biology. *Biochim. Biophys. Acta 811*, 265–322.

(3) Moss, D. A., Leonhard, M., Bauscher, M., and Mäntele, W. (1991) Electrochemical redox titration of cofactors in the reaction center from *Rhodobacter sphaeroides*. *FEBS Lett. 283*, 33–36.

(4) Rappaport, F., Guergova-Kuras, M., Nixon, P. J., Diner, B. A., and Lavergne, J. (2002) Kinetics and pathways of charge recombination in photosystem II. *Biochemistry 41*, 8518–8527.

(5) Lin, X., Murchison, H. A., Nagarajan, V., Parson, W. W., Allen, J. P., and Williams, J. C. (1994) Specific alteration of the oxidation potential of the electron donor in reaction centers from *Rhodobacter sphaeroides*. *Proc. Natl. Acad. Sci. U.S.A. 91*, 10265–10269.

(6) Scheer, H. (1991) *Chlorophylls*, CRC Press, Boca Raton, FL.

(7) Yeates, T. O., Komiya, H., Chirino, A., Rees, D. C., Allen, J. P., and Feher, G. (1988) Structure of the reaction center from *Rhodobacter sphaeroides* R-26 and 2.4.1: Protein-cofactor (bacteriochlorophyll, bacteriopheophytin, and carotenoid) interactions. *Proc. Natl. Acad. Sci. U.S.A. 85*, 7993–7997.

(8) Allen, J. P., Feher, G., Yeates, T. O., Komiya, H., and Rees, D. C. (1987) Structure of the reaction center from *Rhodobacter sphaeroides* R-26: The cofactors. *Proc. Natl. Acad. Sci. U.S.A. 84*, 5730–5734.

(9) El-Kabbani, O., Chang, C. H., Tiede, D., Norris, J., and Schiffer, M. (1991) Comparison of reaction centers from *Rhodobacter sphaeroides* and *Rhodopseudomonas viridis:* Overall architecture and protein-pigment interactions. *Biochemistry 30*, 5361–5369.

(10) Mattioli, T. A., Lin, X., Allen, J. P., and Williams, J. C. (1995) Correlation between multiple hydrogen bonding and alteration of the oxidation potential of the bacteriochlorophyll dimer of *Rhodobacter sphaeroides*. *Biochemistry 34*, 6142–6152.

(11) Nabedryk, E., Allen, J. P., Taguchi, A. K. W., Williams, J. C., Woodbury, N. W., and Breton, J. (1993) Fourier-transform infrared study of the primary electron donor in chromatophores of *Rhodobacter* sphaeroides with reaction centers genetically modified at residue M160 and residue L131. *Biochemistry 32*, 13879–13885.

(12) Rautter, J., Lendzian, F., Shulz, C., Fetsch, A., Kuhn, M., Lin, X., Williams, J. C., Allen, J. P., and Lubitz, W. (1995) ENDOR Studies of the Primary Donor Cation Radical in Mutant Reaction Centers of *Rhodobacter sphaeroides* with Altered Hydrogen-Bond Interactions. *Biochemistry 34*, 8130–8143.

(13) Peloquin, J. M., Williams, J. C., Lin, X., Alden, R. G., Taguchi, A. K. W., Allen, J. P., and Woodbury, N. W. (1994) Time dependent thermodynamics during early electron transfer in reaction centers from *Rhodobacter sphaeroides*. *Biochemistry 33*, 8089–8100.

(14) Kleinfeld, D., Okamura, M. Y., and Feher, G. (1984) Electron-transfer kinetics in photosynthetic reaction centers cooled to cryogenic temperatures in the charge-separated state: Evidence for light-induced structural changes. *Biochemistry 23*, 5780–5786.

(15) Goushcha, A. O., Kharkyanen, V. N., and Holzwarth, A. R. (1997) Nonlinear light-induced properties of photosynthetic reaction centers under low intensity irradiation. *J. Phys. Chem. B 101*, 259–265.

(16) Kálmán, L., and Maróti, P. (1997) Conformation-activated protonation in reaction center of the photosynthetic bacterium *Rhodobacter sphaeroides*. *Biochemistry 36*, 15269–15276.

(17) van Mourik, F., Reus, M., and Holzwarth, A. R. (2001) Long-lived charge separated states in bacterial reaction centers isolated from *Rhodobacter sphaeroides*. *Biochim. Biophys. Acta 1504*, 311–318.

(18) Xu, Q., and Gunner, M. R. (2001) Trapping conformational intermediate states in the reaction center protein from photosynthetic bacteria. *Biochemistry 40*, 3232–3241.

(19) Andréasson, U., and Andréasson, L. E. (2003) Characterization of a semi-stable charge-separated state in reaction centers from *Rhodobacter sphaeroides*. *Photosynth. Res. 75*, 223–233.

(20) Olenchuk, M., and Berezetska, N. (2008) Study of the recombination process of light-induced charge separation in reaction centers of purple bacteria under long-term exposition. *Mol. Cryst. Liq. Cryst. 497*, 121–128.

(21) Deshmukh, S. S., Williams, J. C., Allen, J. P., and Kálmán, L. (2011) Light-induced conformational changes in photosynthetic reaction centers: dielectric relaxation in the vicinity of the dimer. *Biochemistry 50*, 340–348.

(22) Stowell, M. H. B., McPhillips, T. M., Rees, D. C., Soltis, S. M., Abresch, E., and Feher, G. (1997) Light-induced structural changes in photosynthetic reaction center: Implications for mechanism of electron-proton transfer. *Science 276*, 812–816.

(23) Katona, G., Snijder, A., Gourdon, P., Andréasson, U., Hansson, Ö., Andréasson, L. E., and Neutze, R. (2005) Conformational regulation of charge recombination reactions in a photosynthetic bacterial reaction center. *Nat. Struct. Mol. Biol. 12*, 630–631.

(24) Williams, J. C., Alden, R. G., Murchison, H. A., Peloquin, J. M., Woodbury, N. W., and Allen, J. P. (1992) Effects of mutations near the bacteriochlorophylls in reaction center from *Rhodobacter sphaeroides*. *Biochemistry 31*, 11029–11037.

(25) Williams, J. C., Alden, R. G., Coryell, V. H., Lin, X., Murchison, H. A., Peloquin, J. M., Woodbury, N. W., Allen, J. P. (1992) Changes in the oxidation potential of the bacteriochlorophyll dimer due to hydrogen bonds in reaction centers from *Rhodobacter sphaeroides*. *Research in Photosynthesis*, Vol. 1, pp 377−380, Kluwer Academic Publisher, Dordrecht, The Netherlands.

(26) Murchison, H. A., Alden, R. G., Allen, J. P., Peloquin, J. M., Taguchi, A. K. W., Woodbury, N. W., and Williams, J. C. (1993) Mutations designed to modify the environment of the primary electron donor of the reaction center from *Rhodobacter sphaeroides* phenylalanine to leucine at L167 and histidine to phenylalanine at L168. *Biochemistry 32*, 3498–3505.

(27) O'Reilly, J. E. (1973) Oxidation-reduction potential of the ferro-ferricyanide system in buffer solutions. *Biochim. Biophys. Acta 292* 509–515.

(28) Kálmán, L., and Maróti, P. (1994) Stabilization of reduced primary quinone by proton uptake in reaction centers of *Rhodobacter sphaeroides*. *Biochemistry 33*, 9237–9244.

(29) Williams, J. C., Haffa, A. L. M., McCulley, J. L., Woodbury, N. W., and Allen, J. P. (2001) Electrostatic interactions between charged amino acid residues and the bacteriochlorophyll dimer in reaction centers from *Rhodobacter sphaeroides*. *Biochemistry 40*, 15403–15407.

(30) Johnson, E. T., and Parson, W. W. (2002) Electrostatic interactions in an integral membrane protein. *Biochemistry 41*, 6483–6494.

(31) Kálmán, L., LoBrutto, R., Narváez, A. J., Williams, J. C., and Allen, J. P. (2003) Correlation of proton release and electrochromic shifts of the optical spectrum due to oxidation of Tyrosine in RCs from *Rhodobacter sphaeroides*. *Biochemistry 42*, 13280–13286.

(32) Nagarajan, V., Parson, W. W., Davis, D., and Schenck, C. C. (1993) Kinetics and free-energy gaps of electron-transfer reactions in *Rhodobacter sphaeroides* reaction centers. *Biochemistry 32*, 12324–12336.

(33) Wachtveitl, J., Huber, H., Feick, R., Rautter, J., Müh, F., and Lubitz, W. (1998) Electron transfer in bacterial reaction centers with an energetically raised primary acceptor: ultrafast spectroscopy and ENDOR/TRIPLE studies. *Spectrochim. Acta, Part A 54*, 1231–1245.

(34) Kálmán, L., LoBrutto, R., Allen, J. P., and Williams, J. C. (1999) Modified RCs oxidize tyrosine in reactions that mirror photosystem II. *Nature 402*, 696–699.

(35) Kálmán, L., Narváez, A. J., LoBrutto, R., Williams, J. C., and Allen, J. P. (2004) Dependence of tyrosine oxidation in highly oxidizing bacterial RCs on pH and free-energy differences. *Biochemistry 43*, 12905–12912.

(36) McPherson, P. H., Okamura, M. Y., and Feher, G. (1988) Light-induced proton uptake by photosynthetic reaction centers from *Rhodobacter sphaeroides* R-26.1. Protonation of the one-electron states $D^+Q_A^-$, DQ_A^-, $D^+Q_AQ_B^-$, and $DQ_AQ_B^-$. *Biochim. Biophys. Acta 934*, 348–368.

(37) Steffen, M. A., Lao, K., and Boxer, S. G. (1994) Dielectric asymmetry in the photosynthetic reaction center. *Science 264*, 810–816.

(38) Okamura, M. Y., Paddock, M. L., Graige, M. S., and Feher, G. (2000) Proton and electron transfer in bacterial reaction centers. *Biochim. Biophys. Acta 1458*, 148–163.

(39) Woodbury, N. W., Parson, W. W., Gunner, M. R., Prince, R. C., and Dutton, P. L. (1986) Radical-pair energetics and decay mechanisms in reaction centers containing anthraquinones, naphthoquinones, and benzoquinones in place of ubiquinone. *Biochim. Biophys. Acta 851*, 6–22.

(40) Kálmán, L., Gajda, T., Sebban, P., and Maróti, P. (1997) pH-metric study of reaction centers from photosynthetic bacteria in micellular solutions: Protonatable groups equilibrate with the aqueous bulk phase. *Biochemistry 36*, 4489–4496.

(41) Kálmán, L., Williams, J. C., and Allen, J. P. (2003) Proton release upon oxidation of tyrosine in reaction centers from *Rhodobacter sphaeroides*. *FEBS Lett. 545*, 193–198.

(42) Narváez, A. J., Kálmán, L., LoBrutto, R., Allen, J. P., and Williams, J. C. (2002) Influence of the protein environmental on the properties of a Tyrosyl radical in reaction centers from *Rhodobacter sphaeroides*. *Biochemistry 41*, 15253–15258.

(43) Komiya, H., Yeates, T. O., Rees, D. C., Allen, J. P., and Feher, G. (1988) Structure of the reaction center from *Rhodobacter sphaeroides* R-26 and 2.4.1: Symmetry relations and sequence comparison between different species. *Proc. Natl. Acad. Sci. U.S.A. 85*, 9012–9016.

(44) Ermler, U., Fritzsch, G., Buchanan, S. K., and Michel, H. (1994) Structure of the photosynthetic reaction center from *Rhodobacter* sphaeroides at 2.65 Å resolution. Cofactors and protein-cofactor interactions. *Structure 2*, 925–936.

(45) Deisenhofer, J., Epp, O., Miki, K., Huber, R., and Michel, H. (1984) X-ray structure analysis of a membrane protein complex: Electron density map at 3 Å resolution and a model of the chromophores of the photosynthetic RC from *Rhodopseudomonas viridis*. *J. Mol. Biol. 180*, 385–398.

(46) Frolov, D., Marsh, M., Crouch, L. I., Fyfe, P. K., Robert, B., van Grondelle, R., Hadfield, A., and Jones, M. R. (2010) Structural and spectroscopic consequences of hexacoordination of a bacteriochlorophyll cofactor in the *Rhodobacter sphaeroides* reaction center. *Biochemistry 49*, 1882–1892.

(47) Rautter, J., Lendzian, F., Shulz, C., Fetsch, A., Kuhn, M., Lin, X., Williams, J. C., Allen, J. P., and Lubitz, W. (1995) ENDOR studies of the primary donor cation radical in mutant reaction centers of *Rhodobacter sphaeroides* with altered hydrogen-bond interactions. *Biochemistry 34*, 8130–8143.

(48) El-Mashtoly, S. F., Takahashi, H., Kurokawa, H., Sato, A., Shimizu, T., and Kitagawa, T. (2008) Resonance Raman investigation of redox-induced structural changes of protein and heme in the sensor domain of *Ec* DOS protein. *J. Raman Spectrosc. 39*, 1614–1626.

(49) van der Wijk, T., Blanchetot, C., Overvoorde, J., and den Hertog, J. (2003) Redox-regulated rotational coupling of receptor protein-tyrosine phosphatase α dimers. *J. Biol. Chem. 278*, 13968–13974.

(50) Maróti, P., and Wraight, C. A. (1988) Flash-induced H^+ binding by bacterial photosynthetic reaction centers: Influences of the redox states of the acceptor quinones and primary dimer. *Biochim. Biophys. Acta 934*, 329–347.

(51) Fritzsch, G., Koepke, J., Diem, R., Kuglstatter, A., and Baciou, L. (2002) Charge separation induces conformational changes in the photosynthetic reaction center of purple bacteria. *Acta Crystallogr. 58*, 1660–1663.

(52) Shopes, R., and Wraight, C. A. (1986) Primary donor recovery kinetics in reaction centers from *Rhodopseudomonas viridis*. The influence of ferricyanide as a rapid oxidant of the acceptor quinones. *Biochim. Biophys. Acta 848*, 364–371.

(53) van Holde, K. E., Johnson, W. C., Ho, P. S. (2006) *Principles of Physical Biochemistry*, Pearson-Prentice Hall, Upper Saddle River, NJ.